Miscibility and Crystallization Behavior of Poly(ethylene terephthalate)/Poly(ether imide) Blends

Hsin-Lung Chen

Department of Chemical Engineering, Chang Gung College of Medicine and Technology, Kweisan, Taoyuan 33333, Taiwan, Republic of China

Received September 24, 1994; Revised Manuscript Received February 3, 1995[⊗]

ABSTRACT: The miscibility and crystallization behavior of poly(ethylene terephthalate) (PET)/poly(ether imide) (PEI) blends have been investigated by differential scanning calorimetry (DSC) and optical microscopy. PET/PEI blends were prepared by solution precipitation from two solvents: a phenol/tetrachloroethane mixed solvent and dichloroacetic acid. It was found that the compatibility of the as-prepared blends depended on the solvent used. Dichloroacetic acid appeared to provide better segmental mixing for PET and PEI than the mixed solvent of phenol and tetrachloroethane. The compatibility of the blends as prepared from both solvents could be enhanced by melt annealing. The composition dependence of T_g of PET/PEI blends exhibited a cusp at the composition of $w_{PEI} \approx 0.60$ and was analyzed using the classical Gordon–Taylor's equation and the free volume theory of Braun–Kovacs. The PET crystallinity measured from the enthalpy of melting displayed a monotonic drop with increasing PEI content in the composition range of $w_{PEI} > 0.4$, while it stayed approximately constant for $w_{PEI} < 0.4$. The effect of blending with PEI on the multiple melting behavior of PET was also investigated. The highest melting endotherm was found to diminish with increasing PEI content in the blends, showing that the recrystallization of PET after the initial melting was hindered by the presence of PEI. After the crystallization of PET, a strong segregation of PEI was observed. Such segregation of PEI was accompanied with a significant increase in spherulitic nucleation density. The monitoring of the T_g shift during crystallization and the morphological observation by optical microscopy suggested that the crystallization was coupled with a liquid–liquid phase separation, where the miscible melt demixed into the PET-enriched phase and the PEI-rich phase. The morphology created by the liquid–liquid phase separation and the nucleation at the domain interfaces may account for the drastic increase in nucleation density.

Introduction

Poly(ether imide) (PEI), known by the commercial name of Ultem 1000, is a linear amorphous high-performance polymer with a glass transition temperature (T_g) of 215 °C. PEI has the advantages of good mechanical properties and thermal stability, but its solvent resistance is rather poor, which limits its use particularly in aerospace applications.

Poly(ethylene terephthalate) (PET) is a semicrystalline polymer with a T_g of 75 °C and a melting point of ca. 250 °C. PET has been a very important and versatile engineering polymer which has been widely used as fibers, bottles, packages, etc. The relatively low T_g is, however, a potential disadvantage of PET. This may result in a significant decrease in modulus at temperatures between T_g and T_m which limits its use in some applications. In addition, the fast crystallization kinetics is also a negative factor in such a process as bottle production of PET.

A short prior study has reported that PET and PEI were miscible in the melt over the whole composition range.[1] Blending PET with PEI is an alternative to overcome the disadvantages of these two polymers. For example, the presence of PET crystallinity in the blends may enhance the solvent resistance of PEI; in addition, the miscibility increases the T_g of PET and hence lowers its crystallization rate. These examples demonstrate that blending PET with PEI may broaden the application windows of these two polymers.

Because of the potential advantages of PET/PEI blends, more research including the fundamental studies is necessary to provide the structure–property relationship of this binary pair. In this paper, the studies on the miscibility and the crystallization behavior of PET/PEI blends are reported. The solvent-dependent compatibility, crystallization, and melting behavior of this binary pair will be discussed.

Experimental Section

The PET sample used in this study was obtained from Goodyear Tire and Rubber Co., carrying the identification of Vituf. PEI was obtained from General Electric (GE, Ultem 1000), and its molecular weights were $M_n = 12\,000$ and $M_w = 30\,000$.

Blending of PET and PEI was carried out by solution precipitation. Two solvents were used to prepare the blends: a phenol/tetrachloroethane mixed solvent (volume ratio 60/40) and dichloroacetic acid. PET and PEI were dissolved in the phenol/tetrachloroethane mixed solvent at 80 °C, yielding a 4 wt % solution. The blends were subsequently recovered by precipitating them in a 20-fold excess volume of methanol. The blends were washed with a large amount of methanol, followed by drying in vacuo at 100 °C for 5 days. In the case of dichloroacetic acid, the two polymers were dissolved in this solvent at room temperature, followed by precipitating a 10-fold excess volume of water. The blends were washed with a large amount of water and then dried in vacuo at 100 °C for 5 days. The elemental analysis of the dried blends showed less than 0.5 wt % of chlorine content, indicating the nearly complete removal of the solvent.

Thermal transitions of the blends were measured with a Perkin-Elmer DSC-7 differential scanning calorimeter at a heating rate of 20 °C/min. The sample weights were ca. 6.5 mg. The glass transition temperature was obtained from the midpoint of the heat capacity jump, and the cold crystallization temperature (T_c) was considered to be the minimum of the exothermic peak.

The morphologies of PET/PEI blends were observed by a Carl Zeiss cross-polarized optical microscope. Because the compatibility of the as-prepared blends depended on the

[⊗] Abstract published in *Advance ACS Abstracts,* March 15, 1995.

0024-9297/95/2228-2845$09.00/0

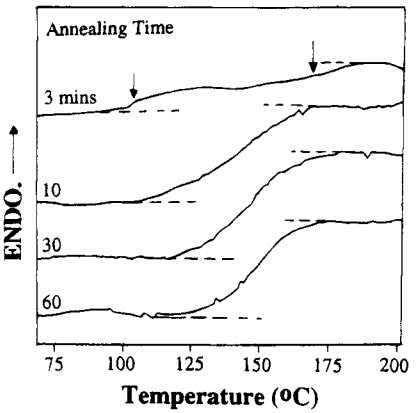

Figure 1. Effect of melt annealing at 280 °C on the glass transition of PET/PEI 40/60 blend prepared from a phenol/tetrachloroethane mixed solvent. The arrows indicate the two T_gs observed for the annealing time of 3 min.

solvent employed in the blend preparation, all the samples used in the optical microscopy study have been homogenized by melt annealing in a DSC at 280 °C for 60 min under a nitrogen atmosphere. After the annealing, the sample under study was sandwiched between two glass slides and was melted on a Thomas Model 40 Micro hot stage at 280 °C for 3 min. The sample was then quickly moved to a Mettler FP2 hot stage preequilibrated at the crystallization temperature, where the resultant morphology was observed.

Results and Discussion

1. Solvent-Dependent Compatibility. A prior study reported that melt-blended PET/PEI was miscible in the melt over the whole composition range.[1] In the present study, PET and PEI were blended by solution precipitation from two solvents, namely, a phenol/tetrachloroethane mixed solvent and dichloroacetic acid. The compatibility of the as-prepared blends was found to depend on the solvent used. Figure 1 displays the glass transition regions of the melt-quenched PET/PEI 40/60 blend prepared from a phenol/tetrachloroethane mixed solvent. The DSC scans were recorded after annealing the as-prepared blends at 280 °C for various time periods. It can be seen that the widths of the T_g regions vary with the melt annealing time at 280 °C. Two T_gs can even be distinguished for the annealing time of 3 min. The T_g width becomes gradually narrower as the annealing was prolonged, showing that the compatibility of the as-prepared blends could be enhanced by melt annealing. Other evidence supporting the improved compatibility by melt annealing is the increase in cold crystallization temperature (T_c) with increasing annealing time. Figure 2 shows the DSC thermograms of the melt-quenched 50/50 blend prepared from a phenol/tetrachloroethane mixed solvent. The T_c moves to a higher value with increasing melt annealing time, indicating that the difficulty of PET crystallization during heating was augmented due to the improvement in compatibility.

The drastic effect of melt annealing on the compatibility of PET/PEI blends as prepared from the two solvents can also be manifested in Figures 3 and 4. Figure 3 displays the composition dependence of T_g of the blends prepared from a phenol/tetrachloroethane mixed solvent. The annealing condition did affect the blend T_g considerably in the composition range of $0.3 \leq w_{PEI} < 0.6$. For the shorter annealing time of 2 and 20 min at 280 °C, the composition variation of T_g exhibits an abrupt jump at $w_{PEI} = 0.5$ and 0.45, respectively. The T_g–composition relationship becomes a typical

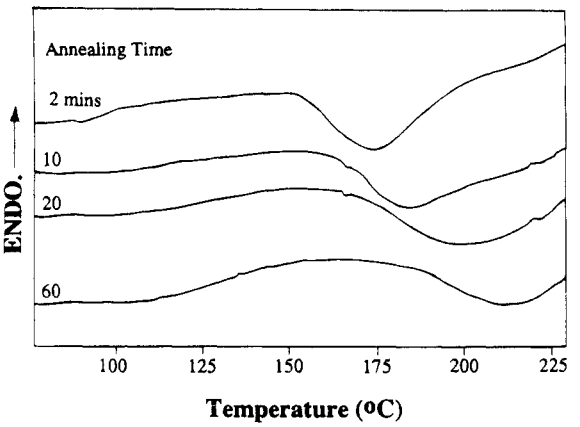

Figure 2. Effect of annealing at 280 °C on the cold crystallization temperature of PET/PEI 50/50 blend prepared from a phenol/tetrachloroethane mixed solvent.

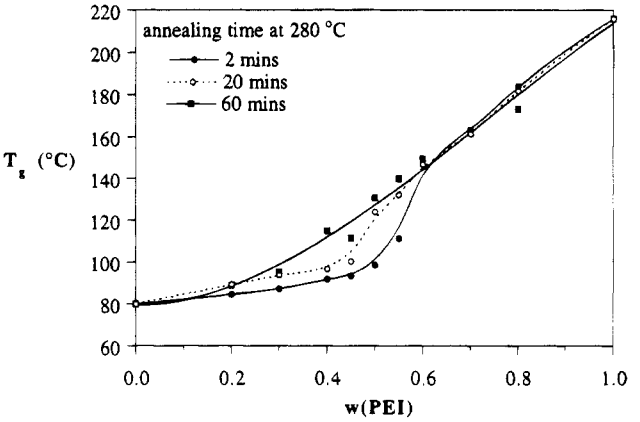

Figure 3. Effect of melt annealing on the composition variation of T_g of PET/PEI blends prepared from a phenol/tetrachloroethane mixed solvent.

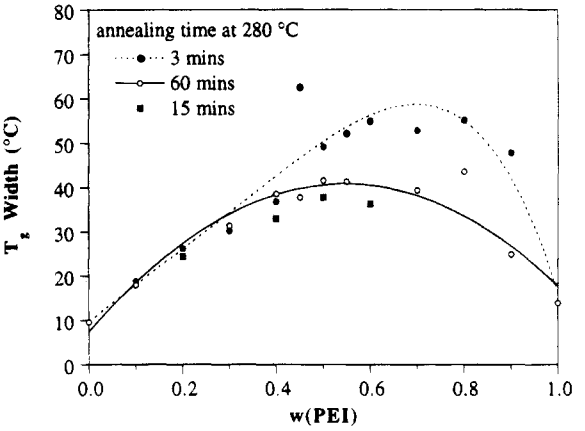

Figure 4. Effect of melt annealing on the composition variation of T_g width of PET/PEI blends prepared from dichloroacetic acid.

monotonic curve after annealing for 60 min. Figure 4 is the composition dependence of T_g widths of blends prepared from another solvent, dichloroacetic acid. The T_g width exhibits a maximum at the intermediate blend composition, which is consistent with the prior paper.[1] The glass transition regions were wider for the shortest annealing time of 3 min, and they became narrower with longer melt annealings for 15 and 60 min. The T_g widths of the blends annealed for 15 min are very close to that of the blends annealed for 60 min, indicating that 15 min of annealing at 280 °C was sufficient to homogenize the blends as prepared from dichloroacetic

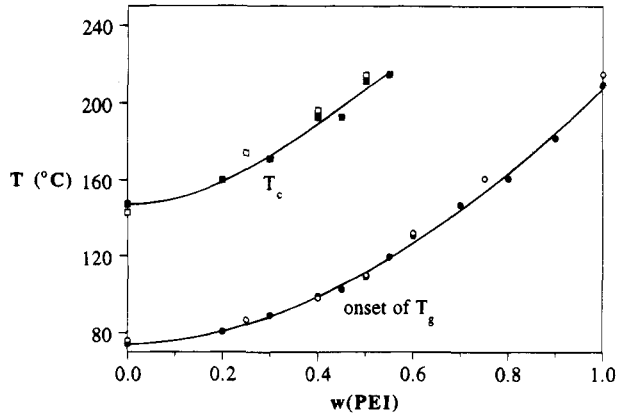

Figure 5. Comparisons of the onset of T_g and the cold crystallization temperature between melt-blended and "homogenized" solution-blended PET/PEI. The closed symbols denote the solution-blended PET/PEI, and the open symbols denote the melt-blended blends.

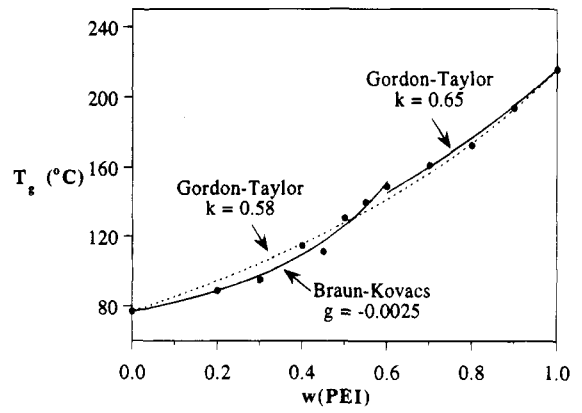

Figure 6. T_g–composition variation of amorphous PET/PEI blends. The solid lines are fits by a combination of Braun–Kovacs and Gordon-Taylor equations, and the dashed line is the fit from Gordon-Taylor's equation.

acid. In the case of the blends as prepared from the phenol/tetrachloroethane mixed solvent, more than 45 min of annealing was required. This suggests that dichloroacetic acid provided better segmental mixing for PET and PEI in the preparation of their binary blends.

It is noted that the chemical stability of PET subjected to the melt annealing at 280 °C should be considered, because the possibility of the undesired thermal degradation and transesterification at high temperature may complicate the observed phase behavior. The possibility of thermal degradation at 280 °C on annealing for 60 min was precluded by thermogravimetric analysis (TGA), which did not indicate any noticeable weight loss for 1 h of annealing under a N_2 atmosphere. In addition, the observation that annealing for more than 60 min at 280 °C did not change T_g, T_c, and T_g width of amorphous PET might also indirectly support this conclusion. PET is known to undergo transesterification with other polyesters such as polyarylate and polycarbonates at high temperature;[2] however, such a reaction between PET and PEI is also precluded because of the great difference between the chemical structures of PEI and polyester and also the high thermal and chemical stability of PEI.

Because the onset of T_g and T_c of the melt-blended PET/PEI have been reported, it is instructive to compare the prior results with that obtained for the "homogenized" blends in the present study. The comparison is displayed in Figure 5. Both the onset of T_g and T_c of the solution-blended PET/PEI agree well with that of the melt-blended blends, which indicates that, after the melt annealing, the solution-blended blends have reached approximately the same homogeneity as that attained in the melt blending.

The results presented thus far have shown that the solvents employed in preparing PET/PEI blends could affect the compatibility between these two polymers. Such a phenomenon has also been observed in several other blends such as polystyrene (PS)/poly(vinyl methyl ether) (PVME).[3,4] Therefore, the effect of solvent-dependent compatibility should be considered in the studies of solution-blended PET/PEI. In the following reported studies, the PET/PEI blends have all been homogenized by annealing at 280 °C for 60 min before further investigations to be carried out. Although it is not known at this stage whether the maximum homogeneity at this temperature has been reached by the 60 min of annealing, the annealed samples should still suffice the DSC studies, because no change in T_g, T_c, and T_g width was observed after further annealing the annealed samples.

2. Composition Dependence of T_g. The composition dependence of T_g has been a great interest in the research of polymer blends. A number of equations, both empirical and predictive, have been proposed to describe the composition variation of T_g,[5-12] and some have related the T_g behavior to the strength of interaction in the blends.[11,12] One of the most frequently used expressions is Gordon–Taylor's equation[5]

$$T_g = \frac{w_1 T_{g1} + k w_2 T_{g2}}{w_1 + k w_2} \tag{1}$$

where k is the adjustable fitting parameter. The composition variation of T_g of amorphous PET/PEI blends is shown in Figure 6. It was found that the T_g–composition variation can be described fairly well by Gordon–Taylor's equation with the value of $k = 0.58$. Nevertheless, it is noted that the T_g difference between PET and PEI is about 140 °C. According to a free volume theory by Kovacs,[7] as the T_gs of the two polymers considered are separated by more than 52 °C, the free volume of the higher-T_g polymer becomes zero at a critical temperature, T_{cr}, and then the classical equations such as the Gordon–Taylor's become invalid below T_{cr} because it would imply a negative free volume, which is impossible. In such a case, the T_g–composition variation exhibits a cusp at the critical composition of ϕ_{1c}. The presence of a cusp in the T_g–composition curve has been observed in some polymer blends such as poly(vinyl chloride) (PVC)/poly(ϵ-caprolactone) (PCL)[13] and PCL/polycarbonate (PC).[14]

If the T_g–composition variation of PET/PEI blends in Figure 6 is reconsidered, a cusp may actually be identified at the composition of $w_{PEI} = 0.6$ (volume fraction = 0.61). According to the Kovacs theory, the critical composition and the critical temperature at which the cusp is located can be calculated by[7]

$$\phi_{1,c} = \frac{f_{g2}}{\Delta\alpha_1(T_{g2} - T_{g1}) + f_{g2}(1 - \Delta\alpha_1/\Delta\alpha_2)} \tag{2}$$

$$T_{cr} = T_{g2} - f_{g2}/\Delta\alpha_2 \tag{3}$$

where the subscript 2 denotes the polymer with the higher T_g, f_{g2} is the free volume fraction of polymer 2 at T_{g2}, and $\Delta\alpha_2$ is the difference between the volume

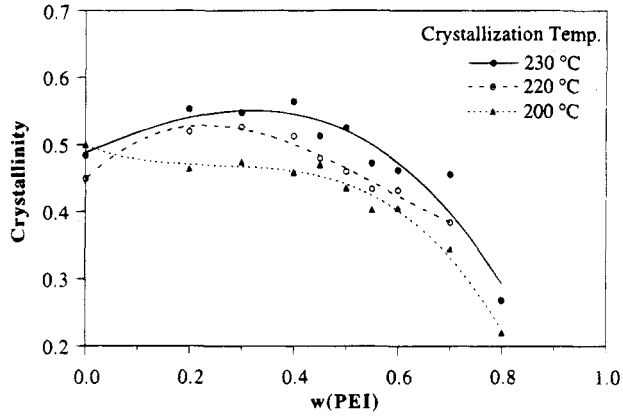

Figure 7. Effect of blending on the PET crystallinity of PET/PEI blends.

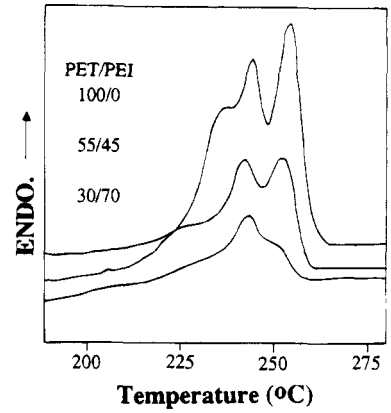

Figure 8. Effect of blending on the PET melting endotherms of PET/PEI blends.

expansion coefficients in the glassy and liquid states. Using the classical values of $f_{g2} = 0.025$ and $\Delta\alpha_1 = \Delta\alpha_2 = 0.000\,48$, the critical composition and temperature of PET/PEI blends were calculated to be $\phi_{1c} = 0.38$ ($\phi_{2c} = 0.62$) and $T_{cr} = 164$ °C. The calculated critical composition is in very close agreement with the experimental value of $\phi_{2c} = 0.61$.

Below T_{cr}, Braun and Kovacs have shown that the composition variation of T_g is given by[8]

$$T_g = T_{g1} + \frac{\phi_2 f_{g2} + g\phi_1\phi_2}{\phi_1\Delta\alpha_1} \qquad (4)$$

where g is an interaction term obtained by fitting the experimental data to eq 4, g is positive if the blend interactions are stronger than the average interactions between the same molecular species, and it is negative otherwise. The Braun–Kovacs equation was used to fit the PET/PEI T_g–composition data below the critical composition, and Gordon–Taylor's equation was applied to the data above ϕ_{2c}. The results are shown in Figure 6. It can be seen that the combination of the Braun–Kovacs and Gordon–Taylor equations can also provide a satisfactory description for the T_g–composition variation of PET/PEI blends. The Braun–Kovacs fit yielded a g of −0.0025. This small negative value suggested that the interaction between PET and PEI was fairly weak.

3. Crystallization Behavior. Since the level of crystallinity is an important factor in determining the polymer properties, it is essential to consider the effect of blending with PEI on the crystallinity of PET. Figure 7 displays the variation of the PET crystallinity with blend composition. The crystallinity reported was determined from the enthalpy of melting (Δh_f), taking 138 J/g as the Δh_f of 100% crystalline PET, and it has been normalized by the weight fraction of PET in the blends. It can be observed in Figure 7 that with increasing w_{PEI} the PET crystallinity stays approximately constant until $w_{PEI} \approx 0.4$, and it drops monotonically thereafter. In general, the crystallization at higher temperature yielded higher crystallinity. Figure 7 shows that blending reduced the crystallizability of PET at moderate to high PEI concentration. Such an effect may arise from the decreased molecular mobility due to the rise in T_g after blending.

The effect of blending on the melting behavior of PET was also evaluated. PET was known to exhibit multiple melting endotherms under normal crystallization conditions.[15–18] Such multiple melting behavior of PET has been ascribed to the simultaneous occurrences of melting, recrystallization, and remelting in the melting region.[15–18] The melting endotherms of PET/PEI blends after crystallization at 200 °C for 15 h are displayed in Figure 8. It is evident that the area of the melting endotherm at 254 °C relative to that at 245 °C becomes smaller with increasing PEI content in the blends. The endotherm at 254 °C even becomes a shoulder of that at 245 °C for the 30/70 blend. This observation can be attributed to the hindrance of PET recrystallization due to the presence of PEI. After the initial melting of the PET crystals, the remixing between PET and PEI took place, and hence the difficulty of the subsequent recrystallization was increased. As a consequence, the relative area of the melting endotherm at 254 °C was decreased. The observation in Figure 8 supports the conclusion that the highest melting endotherm is mainly due to the melting of the PET crystals recrystallized after the initial melting.

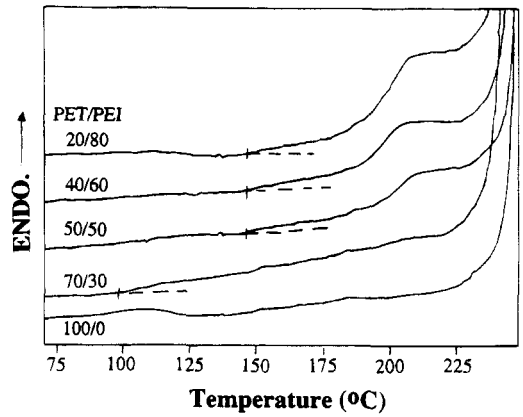

Figure 9. Glass transition regions of PET/PEI blends after crystallizing at 220 °C for 14 h.

The phase behavior and the morphology of semicrystalline PET/PEI blends were also studied here. After the crystallization of PET, a T_g located at ca. 190 °C was clearly observed in the composition range of $w_{PEI} > 0.4$. The T_g regions of PET/PEI blends after crystallization at 220 °C for 15 h are shown in Figure 9. The T_g at ca. 190 °C is clearly identified for the 50/50, 40/60, and 20/80 blends, and it is interesting that this T_g is independent of the initial blend composition. A T_g of 190 °C would correspond to the glass transition which occurred in the amorphous regions containing ca. 85 wt % PEI. Therefore, a strong segregation of PEI appeared to occur during the crystallization of PET. This segregation was also observed at the crystallization temper-

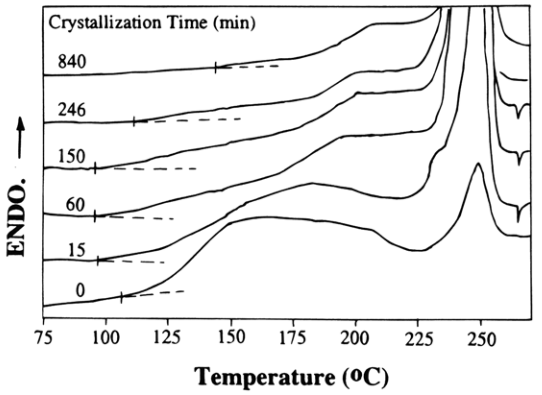

Figure 10. Changes in glass transition regions with crystallization time of PET/PEI 45/55. The crystallization was conducted at 220 °C.

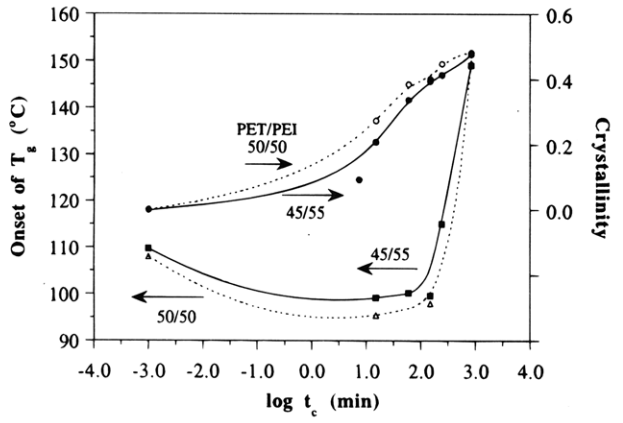

Figure 11. Changes in the onset of T_g and crystallinity with crystallization time of PET/PEI 50/50 and 45/55 blends. The crystallization was conducted at 220 °C.

atures down to 200 °C. For the crystallization temperature lower than 200 °C, the T_g was masked by the melting endotherms, causing its identification in the DSC thermograms to be difficult.

In order to gain a deeper insight on the nature of the PEI segregation, the dynamic annealing experiment was conducted to monitor the change in T_g during the crystallization. In this experiment, the blend sample was annealed at 280 °C for 3 min to erase the previous crystallization history, followed by a crystallization at 220 °C for a time period of t_c. After the crystallization, the sample was quickly quenched into liquid nitrogen to freeze the semicrystalline state thus formed, and then the DSC scan of the quenched sample was recorded. Figure 10 displays the scans of the quenched PET/PEI 45/55 blend. It is seen that the glass transition region did vary considerably during the crystallization. A continuous broadening in the T_g region can be observed in the course of crystallization up to $t_c = 150$ min. The onset of T_g and the crystallinity were plotted against log t_c in Figure 11. The crystallinity increased with increasing t_c, while the onsets of T_g dropped by as many as 10 °C after crystallizing for 150 min from the fully amorphous state. It appears that the PET content was enriched in some amorphous regions during the crystallization, and such a PET enrichment was responsible for the observed T_g decrease. This is somewhat unexpected, because the amorphous PET should always be consumed in the crystallization; such a consumption should lead to an increase in PEI concentration in the miscible amorphous phase, and hence a rise rather than a drop in T_g is expected. The discrepancy can be

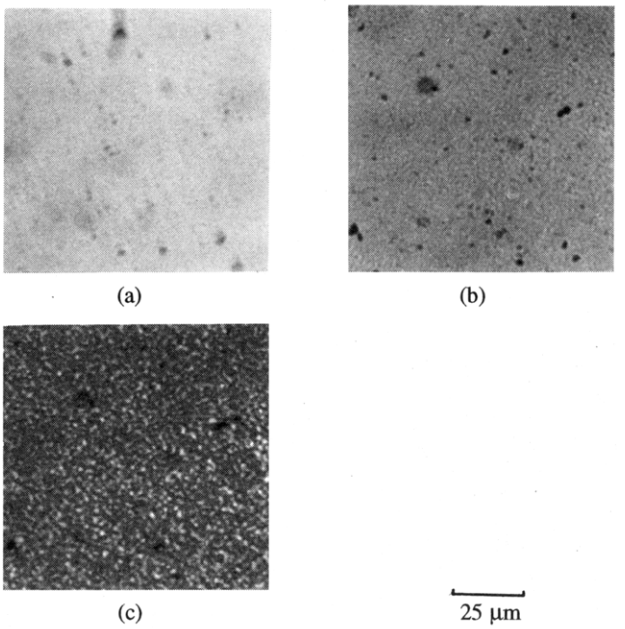

Figure 12. Morphological development of the PET/PEI 60/40 blend annealed at 210 °C for (a) 236, (b) 1038, and (c) 1068 s. Micrographs a and b were observed without cross polarization, and c was observed under cross polarization.

reconciled by proposing that a liquid–liquid phase separation from the miscible melt has taken place simultaneously with crystallization. The miscible melt demixed into the amorphous domains containing more PET than the initial miscible melt (the PET-enriched domains) and the PEI-rich domains. The coupling of the liquid–liquid phase separation with the crystallization can explain both the drop in the onset of T_g and the significant broadening in T_g regions during the crystallization. It is noted that, after the crystallization had proceeded for more than 150 min, the T_g region became narrower, with the onset of T_g moving up to higher temperature. This is due to the occurrence of crystallization in the PET-enriched domains after the liquid–liquid phase separation.

The coupling of crystallization with liquid–liquid phase separation is a rare phenomenon in semicrystalline polymer blends. Such a coupling occurs in the blends whose binodal curves intersect the melting point depression curves.[19–26] Thermodynamically, the binodal curve has no equilibrium significance below the melting point, because crystallization is the favorable phase transformation.[23] Nevertheless, because of the high nucleation barrier in polymer crystallization, formation of a stable nucleus may be preceded by liquid–liquid phase separation.[23] A blend system known to exhibit simultaneous crystallization and liquid–liquid demixing is PS/PCL.[19,22,24] This blend exhibited a UCST, with the PCL melting point curve intersecting the binodal curve.[22,24] Because no liquid–liquid phase separation was observed for PET/PEI blends above the melting point, it is possible that this blend also exhibited a UCST phase diagram, with the binodal curve located below the melting point curve. Further studies on the location of the stability limit (the binodal line) of this binary system are currently underway.

The coupling of liquid–liquid phase separation and crystallization in PET/PEI blends can be further confirmed by observing the morphological development using optical microscopy. Figure 12 displays the result for the 60/40 blend at 210 °C. It can be seen that a

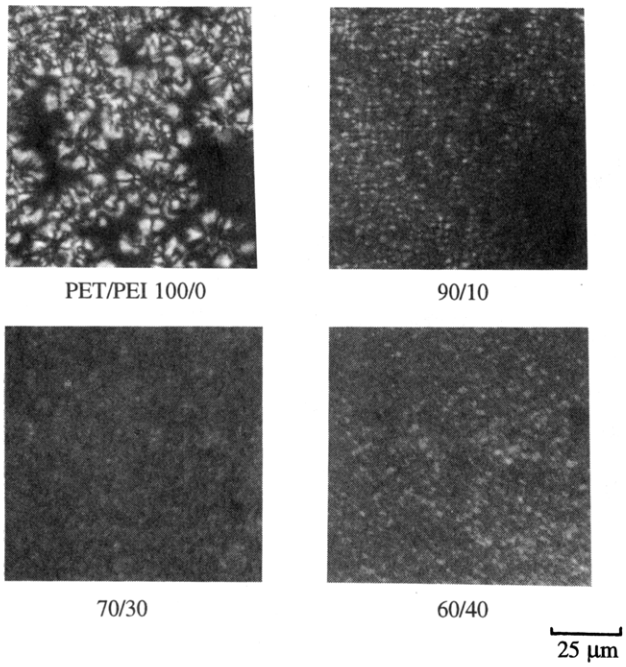

Figure 13. Spherulitic morphologies of PET/PEI blends crystallized at 220 °C.

coarsening structure was formed from the initial homogeneous state. Interestingly, the observed coarsening structure does not appear like the typical spherulite formation; it is indeed similar to the modulated structure developed in the early stage of spinodal decomposition.[26] Therefore, it can be concluded that a liquid–liquid phase separation did take place simultaneously with crystallization. Because both processes occur simultaneously, the liquid–liquid phase separation can compete with crystallization in producing its own morphology, and the final blend morphology is strongly dependent on the outcome of such a competition.[20–25] Inaba et al. have shown that the modulated structure resulting from spinodal decomposition in isotactic polypropylene (i-PP)/ethylene–propylene random copolymer (EPR) blends could be locked in as the crystallization rate of i-PP was sufficiently fast.[20,21] The morphology shown in Figure 12 is indeed such a case where the spinodal modulated structure was conserved throughout the crystallization process. The crystallization of PET from the blend appeared to be sufficiently rapid to compete with the spinodal decomposition to lock in the modulated structure.

Figure 13 compares the final spherulitic morphologies of PET and PET/PEI blends crystallized at 220 °C. The spherulitic nucleation density of the blends was increased prominently, as manifested by the reduction in spherulite sizes. Such a drastic reduction in spherulite size can be ascribed to the morphology created by the liquid–liquid phase separation. Because of high PEI concentration in the PEI-rich domains, the crystallization should take place predominantly in the PET-enriched domains. Further growth of the spherulites in the PET-enriched domains was prohibited as the spherulites impinged the edges of the domains. Therefore, if the sizes of the PET-enriched domains were smaller than the average size of the spherulites grown from pure PET, so were the sizes of the spherulites grown from these domains. In addition to the morphological effect, the nucleation at the domain interfaces may also lead to an increase in nucleation density. It has been suggested that the interfaces of the phase-separated polymer blends may serve as the nucleation sites for crystallization.[27]

Table 1. Crystallization Rate Constants and Avrami Exponents of PET/PEI Blends Crystallized at 220 °C

w_{PEI}	n	k (s^{-1})	w_{PEI}	n	k (s^{-1})
0.0	3.2	0.021	0.4	2.7	0.0018
0.2	2.8	0.0055	0.5	2.9	0.0022
0.3	3.0	0.0038			

Since the nucleation density in the blends was significantly increased, it is interesting to examine whether such an effect has led to some anomalous composition variation of the crystallization kinetics. If the nucleation at the domain interfaces occurred prevalently, the overall crystallization kinetics in the blends may be promoted considerably, and hence the crystallization rate of the blends may be faster than that of the PET homopolymers. Table 1 lists the crystallization rate constants of PET/PEI blends at 220 °C obtained from the Avrami analysis. In spite of the drastic increase in spherulitic nucleation density, the overall crystallization rate of the blends still followed the typical composition variation; i.e., the crystallization rate decreased with increasing PEI composition. This indicates that the nucleation at the interfaces was not a dominant factor in determining the overall crystallization kinetics of PET/PEI blends.

Conclusions

The studies on the solvent-dependent compatibility and the crystallization behavior of PET/PEI blends have been presented in this paper. This binary pair exhibited interesting phase behavior in that the compatibility of these two polymers depended on the solvents employed in the blend preparation. It is thus very important to consider the solvent-dependent compatibility in the investigations of solution-blended PET/PEI. For the two solvents used in this study, dichloroacetic acid appeared to provide better segmental mixing for PET and PEI than the mixed solvent of phenol and tetrachloroethane. The compatibility of the as-prepared blends could be enhanced by melt annealing. The composition dependence of T_g of amorphous PET/PEI blends exhibited a cusp at the composition of $w_{PEI} = 0.6$, which was predicted by a free volume theory of Kovacs. The Braun–Kovacs fit for the T_g–composition variation yielded the interaction term $g = -0.0025$, suggesting that the interaction between PET and PEI was fairly weak.

PET/PEI blends also exhibited very interesting crystallization behavior, which should be a rich area to explore further in the future. The coupling of crystallization with the liquid–liquid phase separation has been observed for this binary blend. Such coupling was accompanied with a significant reduction in spherulite sizes. The reduction in spherulite size has been ascribed to the morphology resulted from the liquid–liquid phase separation and also to the possible nucleation at the domain interfaces. Although the nucleation at the domain interfaces might have taken place in the crystallization, it did not appear to be a dominant factor in determining the overall crystallization kinetics in PET/PEI blends, as the crystallization rate still decreased with increasing PEI.

References and Notes

(1) Martínez, J. M.; Eguiazábal, J. I.; Nazábal, J. *J. Appl. Polym. Sci.* **1993**, *48*, 935.

(2) Porter, R. S.; Jonza, J. M.; Kimura, M.; Desper, C. R.; George, E. R. *Polym. Eng. Sci.* **1989**, *29*, 55.
(3) Bank, M.; Leffingwell, J.; Thies, C. *Macromolecules* **1971**, *4*, 43.
(4) Dana, G. *J. Polym. Sci., Polym. Phys. Ed.* **1984**, *22*, 107.
(5) Gordon, M.; Taylor, J. S. *J. Appl. Chem.* **1952**, *2*, 495.
(6) Fox, T. G. *Bull. Am. Phys. Soc.* **1956**, *1*, 123.
(7) Kovacs, A. *J. Adv. Polym. Sci.* **1963**, *3*, 394.
(8) Braun, G.; Kovacs, A. J. In *Physics of Non-Crystalline Solids*; Prins, J. A., Ed.; North-Holland: Amsterdam, The Netherlands, 1965.
(9) Couchman, P. R.; Karasz, F. E. *Macromolecules* **1978**, *11*, 117.
(10) Couchman, P. R. *Macromolecules* **1978**, *11*, 1156.
(11) Lin, A. A.; Kwei, T. K.; Reisen, A. *Macromolecules* **1989**, *22*, 4112.
(12) Couchman, P. R. *Macromolecules* **1991**, *24*, 5772.
(13) Aubin, M.; Prud'homme, R. E. *Macromolecules* **1988**, *21*, 2945.
(14) Cheung, Y. W.; Stein, R. S. *Macromolecules* **1994**, *27*, 2512.
(15) Holdsworth, P. J.; Turner-Jonas, A. *Polymer* **1971**, *12*, 195.
(16) Roberts, R. C. *Polymer* **1969**, *10*, 117.
(17) Roberts, R. C. *J. Polym. Sci., Polym. Lett. Ed.* **1970**, *8*, 381.
(18) Alfonso, G. C.; Pedemonto, E.; Ponzetti, L. *Polymer* **1979**, *20*, 104.
(19) Tanaka, H.; Nishi, T. *Phys. Rev. Lett.* **1985**, *55*, 1102.
(20) Inaba, N.; Sato, K.; Suzuki, S.; Hashimoto, T. *Macromolecules* **1986**, *19*, 1690.
(21) Inaba, N.; Yamada, T.; Suzuki, S.; Hashimoto, T. *Macromolecules* **1988**, *21*, 407.
(22) Tanaka, H.; Nishi, T. *Phys. Rev. A* **1989**, *39*, 783.
(23) Burghardt, W. R. *Macromolecules* **1989**, *22*, 2482.
(24) Li, Y.; Jungnickel, B.-J. *Polymer* **1993**, *34*, 9.
(25) Lee, H. K.; Myerson, A. S.; Levon, K. *Macromolecules* **1992**, *25*, 4002.
(26) Endres, B.; Garbella, R. W.; Wendorff, J. H. *Colloid Polym. Sci.* **1985**, *263*, 371.
(27) Stein, R. S. *Matter. Res. Soc. Symp. Proc.* **1994**, *321*, 531.

MA946041V